Fabrication of silicon nanowire devices for ultrasensitive, label-free, real-time detection of biological and chemical species

Fernando Patolsky, Gengfeng Zheng & Charles M Lieber

Department of Chemistry and Chemical Biology, Harvard University, 12 Oxford Street, Cambridge, MA 02138, USA. Correspondence should be addressed to C.M.L. (cml@cmliris.harvard.edu).

Published online 16 November 2006; doi:10.1038/nprot.2006.227

© 2006 Nature Publishing Group http://www.nature.com/natureprotocols

Detection and quantification of biological and chemical species are central to many areas of healthcare and the life sciences, ranging from diagnosing disease to discovery and screening of new drug molecules. Semiconductor nanowires configured as electronic devices have emerged as a general platform for ultra-sensitive direct electrical detection of biological and chemical species. Here we describe a detailed protocol for realizing nanowire electronic sensors. First, the growth of uniform, single crystal silicon nanowires, and subsequent isolation of the nanowires as stable suspensions are outlined. Second, fabrication of addressable nanowire device arrays is described. Third, covalent modification of the nanowire device surfaces with receptors is described. Fourth, an example modification and measurements of the electrical response from devices are detailed. The silicon nanowire (SiNW) devices have demonstrated applications for label-free, ultrasensitive and highly-selective real-time detection of a wide range of biological and chemical species, including proteins, nucleic acids, small molecules and viruses.

INTRODUCTION

Nanowire sensor devices

The fundamental principle for detection with semiconductor nanowires[1–3] is their configuration as field-effect transistors (FETs)[4,5], where FETs exhibit a conductivity change in response to variations in the electric field or potential at the surface[2,6,7]. In a standard FET, a semiconductor such as p-type silicon (p-Si) is connected to metal source and drain electrodes through which a current is injected and collected, and the conductance of the semiconductor device is controlled by a third gate electrode capacitively coupled through a dielectric layer[8]. In the case of p-Si, applying a positive gate voltage depletes carriers and reduces the conductance, while applying a negative gate voltage leads to an accumulation of carriers and an increase in conductance. The dependence of the FET conductance on gate voltage also enables direct, electrically based sensing since the electric field resulting from binding of a charged species to the surface is analogous to applying a voltage using a gate electrode. This idea for sensing with FETs was introduced several decades ago for planar FET devices called CHEMFETs[9,10], although the limited sensitivity of these planar devices has precluded them from having as large an impact as chemical or biological sensors.

Silicon nanowires (SiNW) overcome limitations of planar CHEMFETs because the one-dimensional morphology and nanometer-scale cross-section of the nanowires leads to depletion or accumulation of carriers in the 'bulk' of the device when a species binds to the surface (versus only the surface region of a planar device)[7,11–14]. This unique feature of nanowires has yielded sufficient sensitivity to detect single particles[13]. In theory, any semiconductor nanowires can be configured as a FET device for sensing biological and chemical species. However, our work and this protocol focus on silicon nanowires since this material represents one of the best characterized examples of semiconductor nanowires with the structure, size and electronic properties reproducibly controlled[15,16]. Specifically, silicon nanowires can be prepared as single-crystal structures with controllable diameters as small as 2–3 nm[1,2,17], and moreover, as both p-type and n-type materials with well-defined and reproducible high-performance FET device properties[4,5,18]. These reproducible structural and electronic characteristics of the silicon nanowires, which contrast the current state of carbon nanotube devices, are central to their use as the key elements for FET sensors that can be applied in a well-defined and predictable manner to a broad range of biological problems.

A selective sensor can generally be configured from silicon nanowire devices by linking recognition receptor groups to the surface of the nanowire[6,7]. The native silicon oxide coating on silicon nanowires makes this receptor linkage straightforward since extensive data exists for the chemical modification of silicon oxide or glass surfaces from planar chemical and biological sensor literature[19]. When the sensor device with surface receptors is exposed to a solution containing a macromolecule such as a protein, which has a net negative (or positive) charge in aqueous solution, specific binding will lead to an increase (or decrease) in the surface negative charge and an increase (or decrease) in conductance for a p-type nanowire device.

Applications and limitations

A number of protein detection methods exist today, and can be divided into two general categories: label detection and label-free detection. Typical label-based methods involve detection of fluorescence, chemiluminescence or radioactivity from a specific label following target-receptor binding, and include the enzyme-linked immunosorbent assay (ELISA)[20] and nanoparticle labeling assay[21]. The highest sensitivity reported for a labeled detection scheme is in the attomolar range; however, the high-sensitivity of these assays require two antibody receptors, labeling and other manipulation steps that can increase the time and cost of an assay and reduce quantitative accuracy. In addition, these

assays are not suitable for real-time detection and/or kinetic analysis. A number of label-free detection approaches, including surface plasmon resonance (SPR)[22], microcantilevers[23] and carbon nanotubes electronic devices[24], which are based on changes refractive index, bending and conductivity, respectively, have also been described. Specific advances have been made with each of these methods; however, the sensitivity achieved is lower than that reported by fluorescence-based methods. Significantly, none of the label-based or label-free techniques has demonstrated the combination of sensitivity, selectivity, speed and multiplexing achieved by the nanowire devices described in this protocol.

Studies using nanowire field-effect sensors have demonstrated significant advantages for real-time, label-free and highly sensitive detection of a wide range of species, including proteins, nucleic acids, small molecules and viruses, in either single-element or multiplexed formats[25,26], where the key requirement for detection involves a change in charge at the nanowire surface associated with binding and/or dissociation of analyte molecules. This protocol provides an overview and detailed experimental procedure for implementing the label-free nanowire detection/analysis technique, and describes specific examples of applications as well as potential applications of the protocol.

© 2006 Nature Publishing Group http://www.nature.com/natureprotocols

Proteins

Cancer marker proteins have been detected in a multiplexed format down to the femtomolar concentration level with near-perfect selectivity using nanowire sensors modified with monoclonal antibody receptors[14]. In contrast to many optical assays, the detection process is dynamic and reversible, which enables (i) concentration dependent data to be acquired and (ii) cross-binding reactivity to be studied for each device during an experimental run. A potential limitation of the protocol is that the field-effect device detection sensitivity will depend on solution ionic strength. Experiments to date[14] have achieved good response for ionic strengths up to the millimolar level, although the highest sensitivity measurements were carried out in 1–10 μM ionic strength solutions. It is, however, possible to analyze biological samples with minimal sample preparation. Cancer marker proteins have been detected in blood serum samples with 1×10^{11}-fold discrimination versus background serum proteins following a rapid desalting step[14], and marker proteins for renal failure have been detected directly in unpurified urine samples (G.Z., V.S. Vaidya, J.V. Bonventre & C.M.L., unpublished data).

In addition, it is possible to extend protein-based assays in several directions. First, receptors other than antibodies can be used for detection; for example, we have used gangliosides for selective, highly sensitive detection of protein toxins (unpublished data). Linkage of proteins to the nanowire detector surface could also be used to study protein–protein interactions, and small molecule–mediated protein–protein interactions. Second, the nanowire sensors can also be applied to record the dynamics of binding and dissociation, and thereby determine the on/off rate constants and equilibrium association constant for protein-receptor interactions (unpublished data).

Nucleic acids

SiNW field-effect devices have been used for the detection of single-stranded DNA, where recognition of the DNA target molecule was carried out using complementary single-stranded sequences of peptide nucleic acids (PNAs)[11]. PNA was used as the receptor for DNA detection in this work since the uncharged PNA molecule has a greater affinity and stability than corresponding DNA recognition sequences at low ionic strength where nanowire sensitivity is greater. Studies with silicon nanowire devices modified with a PNA receptor designed to recognize wild-type versus the ΔF508 mutation site in the cystic fibrosis transmembrane receptor gene showed that selective detection of wild-type sequences versus sequence with the ΔF508 mutation site could be achieved to the 10 femtomolar level[11].

SiNW sensors have also been used in nucleic acid–based marker assays involving the detection, activity and inhibition of telomerase[14]. The nanowire telomerase assay is remarkably simple: the presence or absence of telomerase is determined by monitoring the nanowire conductance following delivery of a sample cell extract to the device array, and activity is monitored through an increase in conductance resulting from the incorporation of negatively-charged nucleotides near the nanowire surface. Concentration-dependent studies showed that telomerase binding was readily detectable from HeLa cell extracts to at least the ten-cell level without need for PCR amplification, and that the primer-modified nanowires were also effective in monitoring enzymatic activity (i.e., following addition of deoxynucleotide triphosphates)[14]. The capability to measure telomerase activity enabled characterization of the inhibition of telomerase elongation activity in the presence of azido deoxythymidine triphosphate (AZTTP)[14], and suggests that this and related assays could be extended to screening for new inhibitors.

Small molecules

Identification of organic molecules that bind specifically to proteins and macromolecular complexes is central to many areas of the life sciences, and thus represents an important target for sensors. A broadly representative example in this area has been the identification of molecular inhibitors to tyrosine kinases[27]. Nanowire sensor devices were configured for screening small-molecule inhibitors to the kinase Ab1 by linking Ab1 to the surface of the nanowire, and subsequently monitoring the binding of ATP and competitive inhibition of ATP binding with organic molecules[12]. Data recorded from Ab1-modified SiNW devices showed the expected reversible, concentration-dependent increases in conductance upon introducing solutions containing ATP, and importantly, exhibited reversible decreases in conductance because of competitive inhibition of ATP binding by the different small molecules[12].

In addition, we reiterate that the nanowire sensor response is based on change in surface charge or potential (resulting from binding or unbinding), and thus binding of an uncharged small molecule to an immobilized protein or nucleic acid will have a small signal response. The kinase experiments described above, avoided this limitation by using the binding and inhibition of binding of charged ATP to yield a readily measurable and biologically relevant signal change. A similar idea could be implemented to screen for small-molecule inhibitors of protein–protein or protein–nucleic acid binding.

Viruses

SiNW sensor arrays have also been used to selectively detect viruses at the level of a single virus particle[13]. Delivery of very

low concentration influenza A virus solutions, in the order of 80 attomolar (50 viruses per microliter), to p-type SiNW devices modified with monoclonal antibody for influenza A produced well-defined, discrete conductance changes characteristic of binding and unbinding of single positively charged influenza virus[13]. Definitive proof that the discrete conductance changes observed in these studies were due to detection of a single virus binding and then unbinding was obtained from simultaneous optical and electrical measurements using fluorescently labeled influenza viruses, which showed that as a virus diffuses near a nanowire device the conductance remains at the baseline value, and only after binding at the nanowire surface does the conductance drop in a quantized manner similar to that observed with unlabeled viruses; as the virus dissociates and diffuses from the nanowire surface the conductance returns rapidly to the baseline value.

This method was also extended to multiplexing experiments where multiple different nanowire sensor devices were modified with antibody receptors specific to different viruses[13]. Specifically, SiNW devices were modified with monoclonal antibody receptors specific either for influenza A or for adenovirus. Simultaneous conductance measurements obtained when adenovirus, influenza A and a mixture of both viruses were delivered to the devices demonstrated clearly highly selective simultaneous detection of both viruses at the single-virus level. In addition, it should be possible to extend this assay to screen samples simultaneously for larger number of viruses and also exploit different receptors for the viruses.

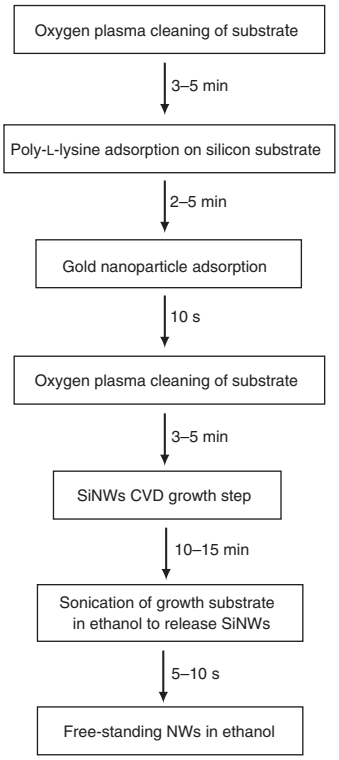

Figure 1 | Flow-chart of steps for the synthesis of silicon nanowires.

Other applications

In addition, we believe it will be possible to adapt the basic protocol to other applications. First, the basic assay format could be extended to much larger array sizes with more sophisticated electronics since the basic sensor chip described in this protocol yields 100–200 independently addressable devices. Larger-scale multiplexing can be implemented using commercially available switching electronics, which can readily monitor tens of devices with good time resolution (unpublished data), and custom electronics can be designed to extend this to much larger size arrays. Second, the SiNW detectors could be developed for a variety of noninvasive cell-based assays. For example, the nanowires and arrays of nanowires can be used as spatially defined local probes of membrane potential relevant to studies of neurons and cardiomyocytes[28].

Experimental overview

The overall steps involved in the synthesis and isolation of SiNWs are shown in **Figures 1** and **2**. The synthesis involves nanoparticle-catalyzed vapor–liquid–solid (VLS) growth on an oxidized silicon

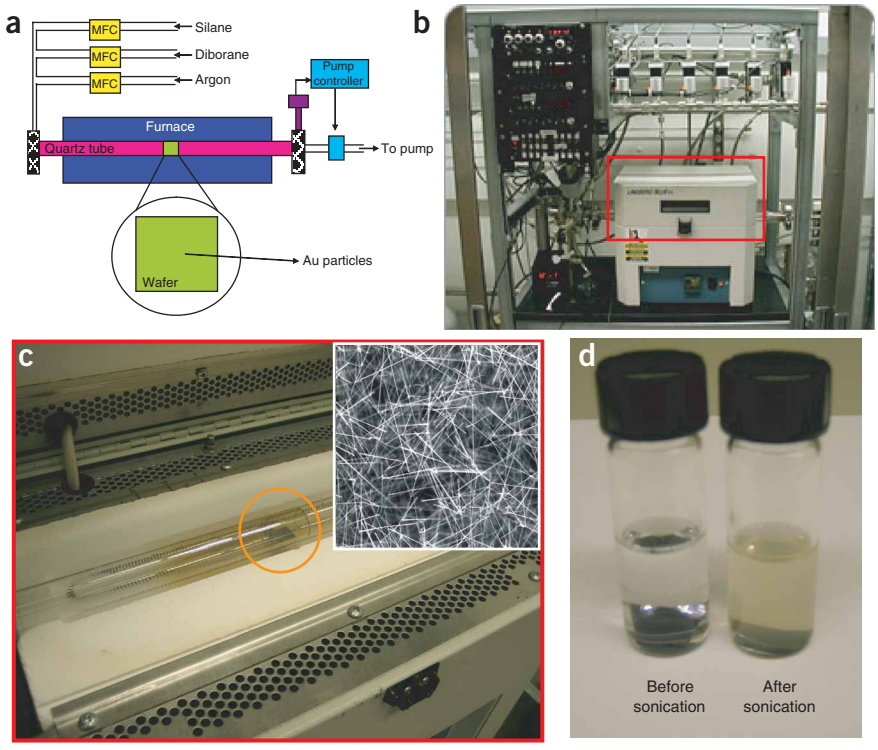

Figure 2 | Synthesis of semiconductor silicon nanowires. (**a**) Scheme of nanowire synthesis set-up. (**b**) Picture of a CVD set-up. (**c**) Center part of the CVD set-up, with a growth wafer sitting inside the quartz tube (circled). SEM images of the grown SiNWs (inset). (**d**) Ethanolic solution before and after sonication in the presence of SiNWs growth wafer (at the bottom of vial).

© 2006 Nature Publishing Group http://www.nature.com/natureprotocols

substrate using gold nanoparticles and silane as the catalyst and silicon reactant, respectively. The diameter of gold nanoparticle catalyst defines the diameter of the resulting SiNWs. The isolation process involves removal of the SiNWs from the substrate into a solution suspension. Following **Figure 1**, the specific steps for SiNW synthesis and isolation are described in Steps 1–9.

The uniformity of the nanowire growth process should be checked by scanning electron microscopy (SEM) imaging of the growth chip (inset, **Fig. 2c**) when reactor conditions are initially optimized. Optimal growth conditions should yield uniform coverage of the nanowires on the growth chip (low-resolution), and uniform nanowire diameters (high-resolution). Transmission electron microscopy (TEM) imaging is also used to check for diameter uniformity during initial optimization.

The steps involved in fabrication of nanowire electronic devices are shown in **Figure 3** and **Figures 4–6**. The fabrication of SiNW FET devices is relatively straightforward compared to conventional planar silicon FET devices, and combines bottom-up assembly of the nanowires on a device chip together with a single step of photolithography to make contacts. Following **Figure 3**, the specific steps for SiNW synthesis and isolation are described in Steps 10–28.

The basic electrical properties of the SiNW devices on the sensor chip are measured as these provide a means for quality control before completion of the sensor device for use. Device measurements in air (**Fig. 7**) are used to identify good devices and any unsuitable devices. Subsequent measurements in aqueous solution (**Figs. 8** and **9**) are not routinely carried out but are useful for testing integrity of good devices identified in air, and is recommended for new users the first time they fabricate sensor chips. The specific steps for SiNW device characterization are described in Steps 29–30.

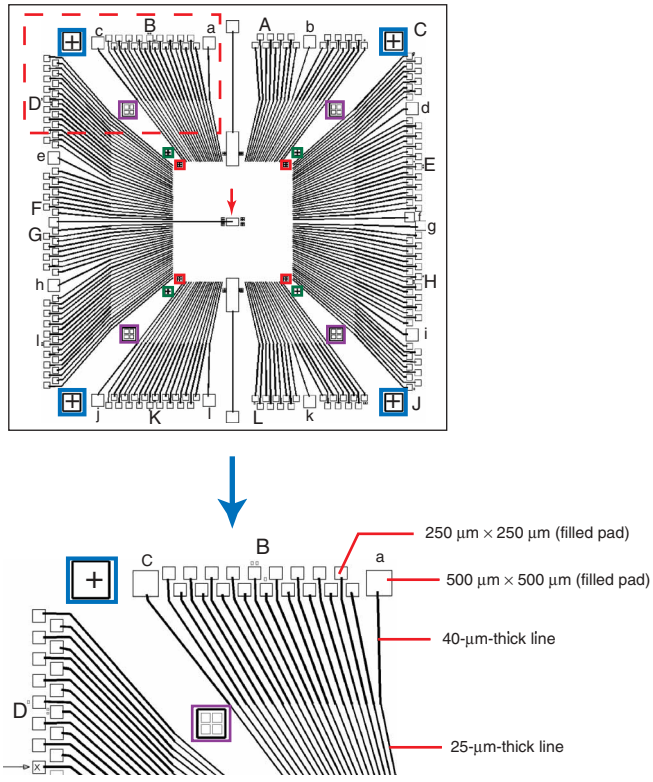

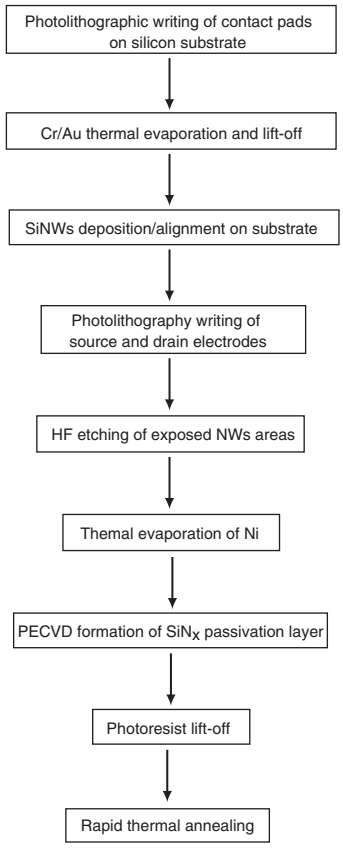

Figure 3 | Flow-chart outlining steps for fabrication of nanowire devices.

For the first time the sensor chip is fabricated by a new user it is advised that the electrical properties of SiNW devices are also measured in aqueous solution. This process allows testing the integrity of the Si_3N_4 passivation, which is essential for stable sensors, and testing of the electronics and microfluidics that will be used in sensor experiments. The overall set-up for solution measurements and sensing are detailed in **Figure 8,** and specific procedures are described in Steps 31–33.

The overall steps involved in linking receptors to the SiNW device surfaces for specific recognition and selective sensing are outlined in **Figures 10** and **11**. The general strategy of covalent linkage of specific receptors to the SiNW device surface involves drawing a solution of receptor into the PDMS channel until the channel is full, allowing the solution to react, and then quenching the reaction. Alternatively, device arrays for

Figure 4 | Photomask pattern for the first photolithography layer. Upper panel: photomask design pattern for the first photolithography layer. (Field of view: 2 × 2 cm chip.) Alignment markers with different magnifications are highlighted with blue, purple, green or red. (This color code is also used for the alignment markers in **Fig. 6** of this protocol.) The red arrow in the pattern center indicates the reference/gate electrode (pad size: 500 × 300 μm, filled). Lower panel: zoom of photomask design pattern from the red rectangle of the upper panel. The dimensions of contact pads and electrode lines are as specified.

© 2006 Nature Publishing Group http://www.nature.com/natureprotocols

multiplexed experiments were made in the same way except that distinct antibody solutions were spotted on different regions of device array/sensor chip. A 5 % v/v glycerol/antibody solution is spotted using a microarrayer (Affymetrix GMS417) with droplet size of ~100 μm. The reactive aldehyde groups on the SiNW surfaces can be used to couple proteins (through lysine residues)[29], and other receptors that have free amine groups.

Following **Figure 10**, the specific steps for surface modification are described in Steps 34–41. As an explicit example we use prostate specific antigen (PSA) monoclonal antibody as a receptor to demonstrate the surface modification procedures and subsequently selective protein (PSA) detection with the devices. The procedure described for PSA antibody can be readily applied to other antibody/antigen pairs since the modification chemistry is quite universal as discussed above.

The expected timing for individual steps in the protocol can be found in **Figures 1, 3** and **10,** and expected timing for the major sections of nanowire synthesis, device fabrication and surface modification are included at the start of the respective sections within the protocol.

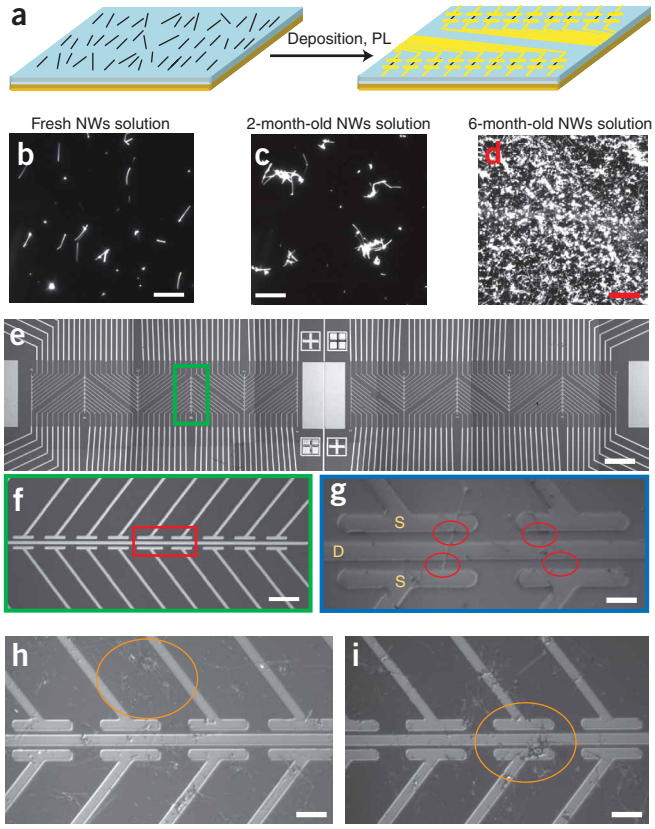

Figure 5 | Nanowire devices and device array fabrication. (**a**) Schematic of deposition of nanowires, and fabrication of nanowire device arrays. PL, photolithography layer. (**b**–**d**) Optical images of SiNWs on silicon wafer samples after the deposition of NWs solution immediately after their synthesis and sonication, after deposition of 2-month-old and 6-month-old nanowire ethanolic solutions, respectively. Scale bars, 20 μm. (**e**) Optical image of the central portion of a device array. White lines correspond to metal electrodes that connect to individual nanowire devices. Scale bar, 120 μm. (**f**) Optical image of one row of addressable device elements from the region highlighted by the green box in **e**. Scale bar, 19 μm. (**g**) DIC optical image of 'good' silicon nanowire devices. The highlighted red circles in **g** indicate the positions of SiNWs between source and drain electrodes (designated as S and D in the figure). Scale bar, 4.5 μm. (**h**,**i**) DIC optical images of poor-quality device chip, as indicated by (i) the low yield of nanowire devices and (ii) the presence of considerable nanowire aggregation on the chip surface. Scale bars, 8.5 μm. The orange circles in **h** and **i** indicate the aggregation of SiNWs and fractures of electrodes.

MATERIALS

REAGENTS

- Silicon wafer substrate for growth and electrical measurement (3′ N100, <0.005 ohm-cm, 356–406 μm thick, with 600 nm thermal oxide, SSP prime grade, Nova Electronic Materials)
- Poly-L-lysine (0.1% w/v aqueous, Ted-Pella)
- Gold nanoparticles, 20 nm diameter (Ted-Pella)
- Gases: silane (99.9+ %, Voltaix), diborane (97 ppm in hydrogen, Voltaix), phosphine (1000 ppm in hydrogen, Voltaix), argon (99%, Matheson Tri-gas), hydrogen (99.9995 %, Matheson Tri-gas) ! **CAUTION** SiH_4, B_2H_6 and PH_3 are toxic. Avoid leakage into air.
- S1805 photoresist (Shipley) ! **CAUTION** Photoresists are irritants. Avoid long exposure time or inhalation.
- LOR3A lift-off resist (MicroChem)
- MF319 developer (Shipley)
- Remover PG solvent stripper (MicroChem)
- Buffered hydrofluoric (HF) acid (fluoride-bifluoride-hydrofluoric acid buffer, Transene) ! **CAUTION** HF is an extremely hazardous liquid and vapor, and is highly corrosive to eyes and skin. Goggles and gloves must be used during operation.
- Gold slug (99.995 %, 3.175 mm diameter × 3.175 mm length, Alfa Aesar)
- Nickel slug (99.995 %, 3.175 mm diameter × 3.175 mm length, Alfa Aesar)
- Chromium-coated tungsten wire (Cr 99.888 %, W 96.5+ %, 1.8 mm diameter × 10 cm length, Alfa Aesar)
- 3-(trimethoxysilyl)propyl aldehyde (90 %, United Chemical Technologies)
- Carbon conductive tape (double coated, 8 mm wide, Ted Pella)
- 0.2 μm cut-off acrodisc syringe filter (0.2 micron HT tuffryn membrane, non-pyrogenic, #4192, Pall).
- Polydimethylsiloxane (SYLGARD 184 silicone elastomer kit, Brownwell)
- Polyethylene tubing (ID/OD, 0.38/1.09 mm, Becton Dickinson)
- Ethanolamine (99.5 %, Sigma)
- Buffer for antibody binding (10 mM phosphate buffer, pH 8.4)
- Buffer for ethanolamine blocking (100 mM ethanolamine in 10 mM phosphate buffer, pH 8.4)
- Buffer for protein sensing (10 μM phosphate buffer, containing 2 μM KCl, pH 7.4)
- Prostate-specific antigen antibody (mouse monoclonal PSA antibody, without bovine serum albumin (BSA) and azides, NeoMarkers)
- Prostate-specific antigen (PSA; EMD Bioscience)
- BSA (New England BioLabs)

EQUIPMENT

- Nanowire chemical vapor deposition (CVD) synthesis apparatus (see **Fig. 2** and EQUIPMENT SETUP)
- Optical microscope (BX51, Olympus)
- Scanning electron microscope (SEM) (LEO982 field emission SEM, Zeiss)
- Transmission electron microscope (TEM) (JEOL2010, JEOL)
- Sonicator (2510, Branson)
- Hotplate (PMC720, Fisher Scientific)
- Spin-coater (PWM32, Headway Research)
- Photolithography mask aligner (2130-C2, AB-M)
- Metal evaporator (Thermal evaporator, Sharon Vacuum)
- Rapid thermal annealer (RTA) (610, Metron Technology)
- Oxygen plasma cleaner (PJ Benchtop, AST Products)
- Plasma-enhanced chemical vapor deposition (PECVD) for silicon nitride deposition (Cirrus-150, Nexx)

© 2006 Nature Publishing Group http://www.nature.com/natureprotocols

- Probe station (TTP-4, Dessert Cryogenics)
- Semiconductor property analyzer (4156C, Agilent)
- Wire-bonder (8850, West Bond)
- Electrical measurment set-up, hardware and software (see **Fig. 8** for details)
- Syringe pump for sample delivery (PhD2000, Harvard Apparatus)
- Lock-in amplifier (SR830, DSP dual-phase, Stanford Research Systems)
- Current pre-amplifier (1211, DL Instrument)
- Multifunction I/O adaptor panel (BNC-2090, National Instrument)
- DAC card (PCI-6030E, National Instrument)

EQUIPMENT SETUP

Nanowire synthesis system The homebuilt SiNW CVD synthesis apparatus (**Fig. 2**) includes several basic subsystems: (i) gas delivery subsystem; (ii) reactor subsystem; and (iii) pumping subsystem. (i) The delivery of reactants is accomplished using mass flow controllers (MFCs, 1179A21CR1BV-S, MKS Instrument) which are controlled electronically using MKS 247D controller. The MFCs are connected together and to the gas sources and reactor with stainless steel tubing using VCR fittings. The subsystem must be leak free, which we assess by pumping to 1×10^{-6} torr. (ii) The reactor consists of a tube furnace (TF55035A, Lindberg/Blue) for controlling of the nanowire growth temperature and a removable 25 mm quartz tube. The ends of the quartz tube are connected to the gas delivery and pumping subsystems using 25 mm O-ring sealed stainless steel connectors, which can be readily attached and removed from the quartz tube ends. (iii) The overall pumping systems must be based on a vacuum pump that is compatible with reactive gases; in our system a dry pump (SD60VII, Kashiyama) is used. The pressure within the quartz reactor is controlled using a combination of a capacitance pressure gauge (626A13TBE, MKS Instrument) for monitoring reaction pressure, an automated valve (148A14C1AM, MKS Instrument), for varying gas flow to the pump, and an electronic pressure controller (MKS 250E-4-D, MKS Instrument) for maintaining pressure of the system at fixed value (via input from pressure gauge and output to valve).

Microfluidic channel The microfluidic delivery device was fabricated using reported procedures[30] from polydimethylsiloxane (PDMS). The overall dimension of the PDMS is ~10 × 10 × 5 mm (length × width × height), and the fluidic channel is 5 × 0.5 × 0.05 mm. The ~0.7 mm diameter inlet and outlet holes are located at the two ends of the channel. The fabrication process in brief is as follows: (i) Fabrication of channel master. Spincoat SU-825 (Shipley) on a silicon wafer at 500 r.p.m. for 5 s and 850 r.p.m. for 15 s, and then bake at 95 °C for 50 min. This process yields an ~0.05-mm-thick layer of the photoresist. Expose the channel pattern for 15 s using photolithography followed by baking at 95 °C for 4 min. The SU-825 surrounding the channel is dissolved using propylene glycol methyl ether acetate (PGMEA, Sigma) for 5 min, rinsing with PGMEA, and then drying with nitrogen gas. (ii) Fabrication of the PDMS delivery device. Place the master in a clean 7.5-cm-diameter Petri dish, and then pour over a fully-stirred mixture of 40 g Sylgard-184 silicone elastomer and 4 g Sylgard-184 silicon elastomer curing agent (Dow Corning). After standing for ~20 min, place the Petri dish in a dessicator and evacuate with house vacuum for 2 h (to remove all gas bubbles), and then bake the Petri dish at 80 °C for 6 h. Peel the cured PDMS off the master and then cut to the final device dimensions around the channel.

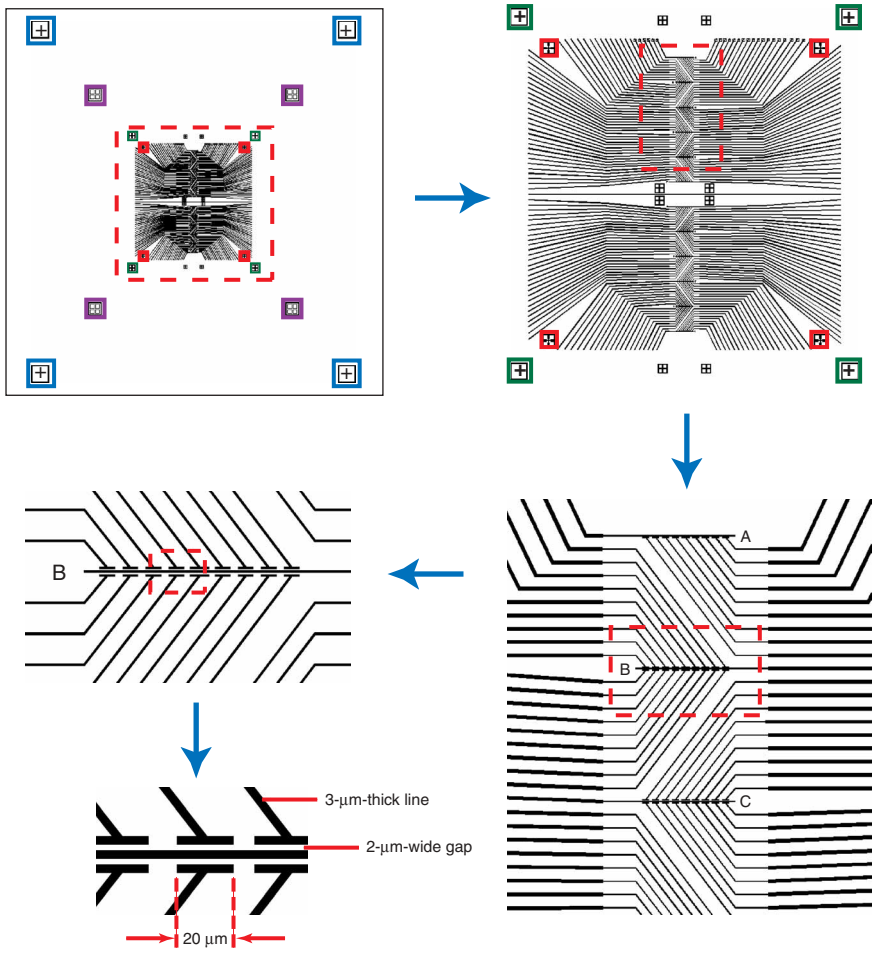

Figure 6 | Different magnifications of the photomask design pattern for the second photolithography layer. Alignment markers with different magnifications are highlighted with blue, purple, green and red colors, respectively (color code is the same as for alignment markers in **Fig. 4**). Each panel following the arrow corresponds to a zoomed image from the red rectangular region in the previous panel. The dimensions of the thinnest electrode lines and FET device channels are as specified.

PROCEDURE

Nanowire synthesis and isolation ● TIMING 1–2 h

1| Clean the silicon dioxide (SiO_2) surface of a 1 × 2 cm^2 piece of silicon wafer (the growth chip) with oxygen plasma: 100 W and 50 sccm (standard cubic centimeters per minute; 1 sccm = 1.7×10^{-8} m^3 s^{-1}) O_2 for 200 s. This plasma treatment removes organic residues and makes the surface hydrophilic.

2| Place the chip on a flat and clean surface (it is not necessary to place inside container). Cover the clean surface of the growth chip with a 0.1% poly-L-lysine (~200 μl), and allow the solution to stand for 2 min.

3| Remove the poly-L-lysine by rinsing with a stream of dH_2O from a squeeze bottle for 5 s (~10 ml), and then dry the surface using a gentle stream of nitrogen gas for 10 s.

© 2006 Nature Publishing Group http://www.nature.com/natureprotocols

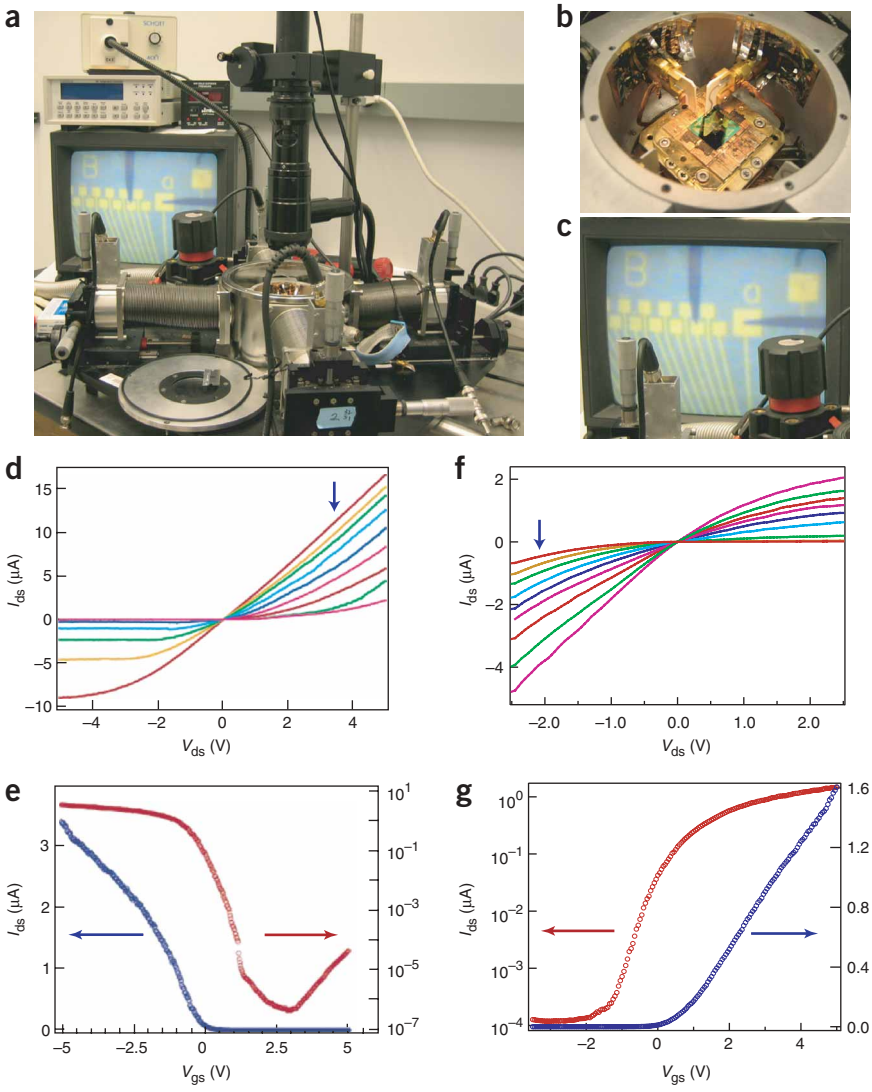

Figure 7 | Transport measurement of SiNW devices in air. (**a**) Probe station for electrical transport measurement of SiNW device chip. (**b**) Chamber of the probe station where the SiNW sensor chip is located and connected to different probes. (**c**) Monitor used for locating the electrode pads that the measurement probes connect to. (**d**) Family of source-drain current (I_{ds}) versus source-drain voltage (V_{ds}) plots at different gate voltages for a typical p-type SiNW FET. The red, orange, green, cyan, blue, magenta, red, green and magenta curves (as follow the direction of the arrow) correspond to gate voltage (V_g) values of −5, −4, −3, −2, −1, 0, 1, 2, and 3 V, respectively. (**e**) I_{ds} versus V_g recorded for the same p-type SiNW FET device in **d** plotted on linear (blue) and logarithmic (red) scales at a V_{ds} of 1 V. (**f**) Family of source-drain current (I_{ds}) versus source-drain voltage (V_{ds}) plots at different gate voltages for a typical n-type SiNW FET. Different V_g values (−5, −4, −3, −2, −1, 0, 1, 2 and 3 V) were plotted using the same color code as in **d**. (**g**) I_{ds} versus V_g recorded for the same n-type SiNW FET device in **f** plotted on linear (blue) and logarithmic (red) scales at a V_{ds} of 1 V.

4| Cover the growth chip surface with a solution of 20 nm gold nanoparticles (diluted 1:4, v/v with dH_2O; final concentration ~ 2×10^{11} particles per ml), allow the solution to stand for 10 s and then rinse the surface with a stream of dH_2O for 5 s (~10 ml). Dry the surface using a gentle stream of nitrogen gas for 10 s. The negatively charged gold nanoparticles are electrostatically bound to the positively charged poly-L-lysine-covered growth chip surface.

▲ **CRITICAL STEP** It is important to use freshly diluted nanoparticle solution and to keep the nanoparticle deposition time to ~10 s to avoid aggregation of gold, which will produce a broad range of nanowire diameters.

5| Clean the gold nanoparticle growth chip in an oxygen plasma: 100 W and 50 sccm O_2 for 5 min. The cleaning step enables uniform nucleation and nanowire growth.

6| Place the clean growth chip in the middle of the quartz reactor tube inside the CVD growth furnace (**Fig. 2c**).

7| Evacuate the reactor to less than 3 mtorr and increase the temperature to 460 °C in a 10 sccm Ar flow and a total pressure of 10 mtorr.

8| When growth temperature is stable, introduce silane (SiH_4), which is the silicon reactant source, and dopant–diborane (B_2H_6) for p-type and phosphine (PH_3) for n-type nanowires–into the reactor. The typical growth conditions for p-type SiNWs are 10 sccm Ar, 6 sccm SiH_4, 7.5 sccm B_2H_6 (97 ppm in H_2), total chamber pressure 25 torr, temperature of 460 °C, and growth time of ~10 min, where typical growth rate is 1.2-1.5 μm min^{-1}. The typical growth conditions for n-type SiNWs are 30 sccm H_2, 8 sccm SiH_4, 2 sccm PH_3 (1000 ppm in H_2), total chamber pressure 40 torr, temperature of 460 °C, and growth time of ~15 min, where typical growth rate is 0.8-1.0 μm min^{-1}. At the end of the growth, terminate the reactant flow and evacuate the reactor tube (3 mtorr). Shut down the furnace and open for cooling (~30 min). During initial optimization, the nanowires should, at this stage, be checked by SEM and TEM.

! **CAUTION** SiH_4, B_2H_6 and PH_3 are toxic. Avoid leakage into air.

■ **PAUSE POINT** The nanowire growth chips are stable in a dry environment.

? **TROUBLESHOOTING**

© 2006 Nature Publishing Group http://www.nature.com/natureprotocols

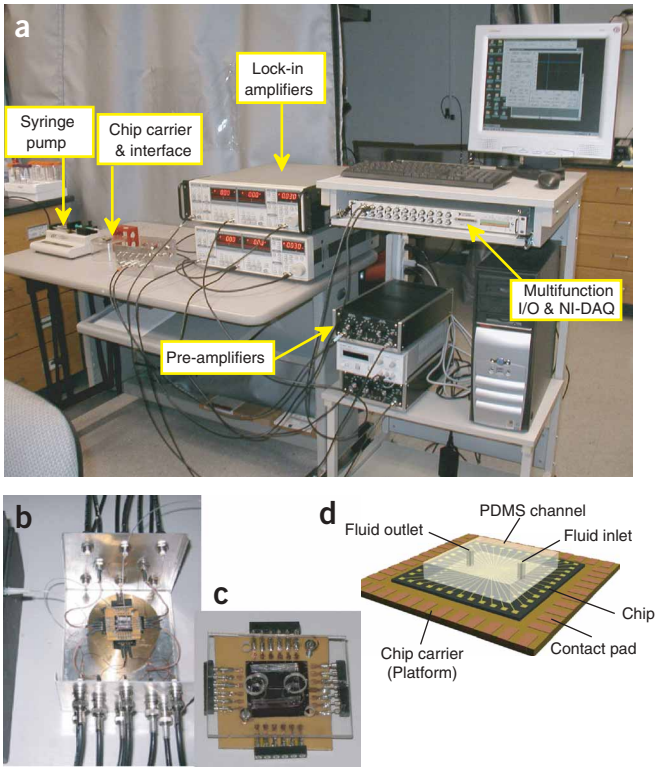

Figure 8 | Nanowire FET sensing set-up. (**a**) An electrical measurement setup. The solution is delivered by the microfluidic channel and a syringe pump. (**b,c**) Optical images at different magnification of the nanowire sensor biochip with integrated microfluidic sample delivery and (**d**) Schematic of a the prototype nanowire sensor biochip with integrated microfluidic sample delivery as shown in **c**. (**e**) Schematic of the sensing set-up including the electronic components and their electrical connections.

9| Remove the nanowires from the growth chip and suspend in 1–2 ml of ethanol by sonication for 5–10 seconds. The ethanol suspension of SiNWs is a transparent yellow-brown color as shown in **Figure 2d**. The nanowire solution should be checked for uniformity by placing a drop onto a silicon chip, and imaging by SEM. Chips imaged by SEM should not be used subsequently for devices, because contaminants can be deposited onto the nanowire surfaces during the imaging process.

■ **PAUSE POINT** The nanowire solutions can be stored for 1-2 weeks but do degrade with time.

? TROUBLESHOOTING

Nanowire-device fabrication and electrical characterization ● TIMING 6–8 h

10| Clean the silicon dioxide (SiO_2) surface of a 2 × 2 cm^2 piece of silicon wafer (the sensor chip) with oxygen plasma: 100 W and 50 sccm O_2 for 200 s.

11| Deposit a two-layer photoresist consisting of LOR3A and S1805 onto the sensor chip by spin coating: (i) Deposit 0.5 ml LOR3A by spinning at 500 rpm for 5 s then 4000 rpm for 40 s, followed by baking at 185 °C on a hotplate for 5 min; the LOR3A layer thickness should be ~300 nm. (ii) Deposit 0.5 ml S1805 by spinning at 500 rpm for 5 s then 4000 rpm for 40 s, followed by baking on a hotplate at 115 °C for 90 s; the S1805 layer thickness should be ~500 nm.

! CAUTION Photoresists are irritating. Avoid long-time exposure or inhalation.

▲ CRITICAL STEP Photoresist deposition, photolithography, developing and metal deposition should be carried out in a clean room (Steps 11–15).

12| Define the outer contact pads and interconnects by photolithography (wavelength 350–430 nm, exposure time 0.8 s) using the photomask shown in **Figure 4**.

13| Use tweezers to clamp the edge of the chip and hold it firmly. Immerse the photopatterned chip in MF319 developer for 1 min, and then rinse by immersing in dH_2O (30–50 ml) with gentle agitation for 1 min. Dry the chip in a stream of nitrogen gas for 30 s.

14| Clean the sensor chip using an oxygen plasma: 30 W and 50 sccm O_2 for 60 s, and place it in a thermal evaporator.

15| Evacuate the evaporator chamber until it reaches a base pressure in the 10^{-7} torr range and define the contact pads by sequentially depositing chromium and gold. To achieve this, deposit 5 nm of chromium at 0.1 nm s^{-1} followed immediately by 60 nm of gold at 0.1 nm s^{-1} within the multi-source thermal evaporator.

16| Dissolve off the remaining resist with immersion in 20–30 ml Remover PG at 70 °C for 30 min. Wash with (i) acetone and (ii) ethanol for 5–10 s each using squeeze bottles, and then dry for 10 s in a stream of nitrogen gas.

© 2006 Nature Publishing Group http://www.nature.com/natureprotocols

■ **PAUSE POINT** Chips with outer metal contact pads can be stored in a desiccator for later use (should be used within 1 week).

17| The sensor chip with outer metal contact pads is cleaned using an oxygen plasma: 100 W and 50 sccm O_2 for 200 s.

18| Deposit the nanowire-containing ethanol solution drop-wise on the clean oxide surface of the sensor chip using 1 µl aliquots (~20 drops in total). Deposit the drops in the central region of the chip where the devices will be made, and allow each drop to evaporate before the next drop is deposited. The optimal nanowire density for device design used in the sensor chips is 1–2 nanowires per 100 μm^2, where nanowire density is observed by dark-field optical microscopy (**Fig. 5b**). Because nanowires will aggregate in solution over time it is advised that solutions ≤2 weeks old are used for deposition. (Alternatively, the SiNWs can be aligned on the growth chip by using solvent flow-induced alignment[31] or Langmuir-Blodgett[5,32] methods. These methods, however, require much larger quantities of SiNWs and are technically more demanding than simple pipette deposition.)

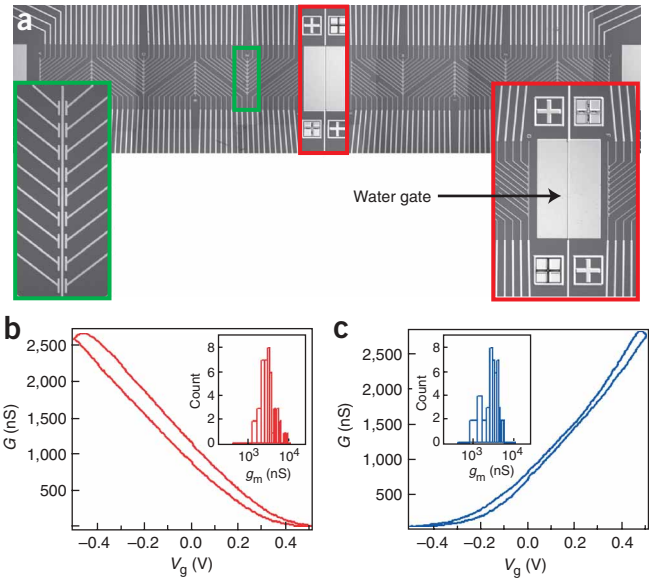

Figure 9 | Optical images of device array and transport of SiNW devices in aqueous solution. (**a**) Optical image of the central portion of a device array. White lines correspond to metal electrodes that connect to individual nanowire devices. (Left inset) Optical image of one row of addressable device elements from the region highlighted by the green box in **a**. (Right inset) Optical image of the 'water gate' electrode on the array from the region highlighted by the red box in **a**. (**b**,**c**) Electrical properties of SiNW FETs in aqueous solution. (**b**) Water-gate transconductance of a p-type SiNW. (Inset) Histogram of transconductance values of more than 50 p-type SiNW devices. (**c**) Water-gate transconductance of an n-type SiNW. (Inset) Histogram of transconductance values of more than 50 n-type SiNW devices.

▲ **CRITICAL STEP** Uniform dispersion of the nanowires in the central region of the sensor chip at a density matched to the metal electrode size or spacing is important for achieving a high yield of reproducible SiNW devices.

? TROUBLESHOOTING

19| Deposit a two-layer photoresist consisting of LOR3A and S1805 onto the sensor chip by spin coating as described in Step 11.

20| Define the source/drain electrodes and inner interconnects by photolithography (wavelength 350–430 nm, exposure time 0.8 s) (**Fig. 5a**) using the photomask shown in **Figure 6**. Using an optical microscope align the photomask to the pattern defined in Step 12 using common alignment markers (**Figs. 4** and **6**).

21| Immerse the photopatterned chip in MF319 developer for 1 min, and then rinse by immersing in dH_2O (30–50 ml) with gentle agitation for 1 min. Dry the chip in a stream of nitrogen gas for 30 s.

22| Clean the sensor chip using an oxygen plasma: 30 W and 50 sccm O_2 for 60 s.

23| Immediately before placing the sensor chip in the metal evaporator, etch the contact regions in buffered hydrofluoric acid (HF) solution to remove oxide on the SiNW surface. Immerse the chip completely in HF solution for 5–8 s, then in 30 ml dH_2O for 10 s. Dry for <10 s in a stream of nitrogen gas, and then immediately place in the metal evaporator.

! **CAUTION** HF is extremely hazardous liquid and vapor, and is highly corrosive to eyes and skin. Goggles and gloves must be used during operation.

▲ **CRITICAL STEP** The removal of oxide from the SiNW surface is crucial for obtaining a good metal–silicon electrical contact. Once the surface oxide is removed by HF it is important to place the sensor chip into and evacuate the metal evaporator, because oxide will re-form on the silicon surface in air. It is also important not to etch the surface longer than necessary, since HF will also remove oxide from the substrate.

24| Evacuate the evaporator chamber until it reaches a base pressure in the 10^{-7} torr range, and then deposit 60 nm Ni at 0.1 nm s^{-1} to define the source/drain contacts and inner interconnectors.

25| After Ni deposition remove the sensor chip from the evaporator and transfer immediately to the PE-CVD chamber for silicon nitride deposition. The Si_3N_4 passivation layer is 20–30 nm thick and deposited with the following conditions: Ar (20 sccm), SiH_4 (40 sccm, 3% in Ar), N_2 (6 sccm), total chamber pressure of 5 mtorr, microwave power of 375 W and a deposition time of 600 s.

© 2006 Nature Publishing Group http://www.nature.com/natureprotocols

26| Dissolve off the remaining resist by immersion in 20–30 ml Remover PG at 70 °C for 30 min. Wash with (i) acetone and (ii) ethanol for 5–10 s each using squeeze bottles, and dry for 10 s in a stream of nitrogen gas.

27| Anneal the metallized sensor chip using a rapid thermal annealer at 380 °C for 2 min in forming gas (10% H_2/90% N_2) to form low-resistance NiSi contacts[33] at the interfaces between the SiNWs and source/drain Ni electrodes.

28| Examine sensor chips upon completion of annealing by optical microscopy. Metal contact pads, interconnection lines and source drain contacts should appear well-formed, continuous and sharp with a good yield of single SiNWs spanning source/drain electrodes as shown in **Figure 5e–g**. Sensor chips with a low yield of nanowire devices, considerable nanowire aggregation and/or poorly defined or broken metal lines (**Fig. 5h,i**) should be discarded.

■ **PAUSE POINT** Nanowire device chips can be stored in a desiccator for later use (should be used within 1 week).

▲ **CRITICAL STEP** It is important to use sensor chips that exhibit well-formed, continuous, and sharp metal contact pads, interconnection lines and source drain electrodes, as well as a good yield of single SiNWs spanning source or drain electrodes because these characteristics are indicative of good lithography/metallization and uniform SiNW dispersion, respectively. Sensor chips without these characteristics will tend to exhibit irreproducible electrical characteristics and poor sensor behavior.

? TROUBLESHOOTING

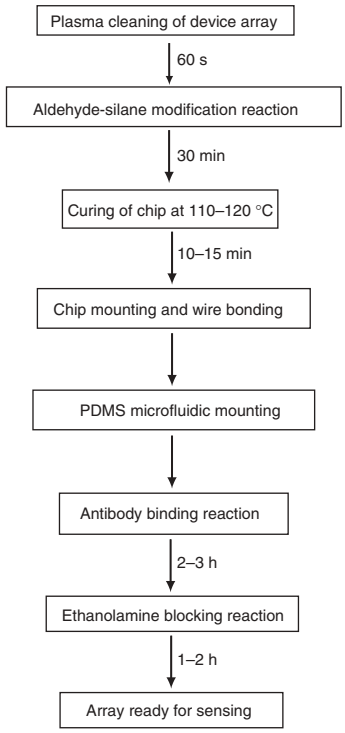

Figure 10 | Flow-chart of chemical modification steps used to link receptors to the surfaces of silicon nanowire devices.

29| For air characterization, connect individual SiNW devices on the sensor chip to measurement electronics (semiconductor property analyzer) using a probe station (**Fig. 7a–c**). Bring probes into contact with the outer metal contact pads on the sensor chip, while viewing optically (**Fig. 7c**).

30| Test individual SiNW devices on the chip to identify suitable and unsuitable devices. The current (I_{ds}) versus drain-source voltage (V_{ds}) for several gate voltages (V_{gs}) and I_{ds} versus V_{gs} for $V_{ds} = 1$ V are typically measured. Data representative of suitable p-type and n-type SiNW devices are shown in **Figure 7d,e** and **Figure 7f,g**, respectively.

▲ **CRITICAL STEP** Electrical characteristics similar to those shown in **Figure 7** provide a reliable indicator for subsequent good sensor performance. It is important to optimize device fabrication to achieve this level of performance before proceeding.

? TROUBLESHOOTING

31| Mount the sensor chip on a chip-carrier using double-sided conductive carbon tape, and then use wire bonding to connect contact pads of good devices to the 24 output pads of the chip carrier (**Fig. 8b–d**). This enables ~ 11 devices and a reference or gate electrode to be connected, although a larger number of devices is possible with shared source electrodes.

32| Clamp a single channel microfluidic device on the chip carrier such that the channel overlaps the central region of the sensor chip, which contains the SiNW devices (**Fig. 8c,d**), and draw solution (10 μM phosphate buffer, containing 2 μM KCl, pH 7.4) into the channel through 0.38 mm ID polyethylene tubing attached to the inlet using a syringe pump attached to the channel outlet using the same size tubing. Typical flows used in experiments are 0.3–0.4 ml h^{-1}.

33| Characterize individual SiNW devices in aqueous buffer solution (10 μM phosphate buffer, containing 2 μM KCl, pH 7.4) by measuring the conductance, G ($= dI_{ds}/dV_{ds}$) as a function of the water gate potential, V_g. G is measured in these and sensor experiments using a lock-in technique (**Fig. 8a,e**), where V_{ds} is modulated at 79 Hz with a 30 mV amplitude and $V_{ds}(dc) = 0$ V, and the water gate electrode is located centrally within the sensor chip device array (**Fig. 8e** and **Fig. 9a**). Data representative of suitable p-type and n-type SiNW devices are shown in **Figure 9b** and **c**, respectively. The yield of nanowire devices calculated based on all of the available source/drain electrodes is normally 30–50%.

© 2006 Nature Publishing Group http://www.nature.com/natureprotocols

■ **PAUSE POINT** Nanowire device chips can be stored in a desiccator for later use (should be used within 1 week).
? TROUBLESHOOTING

Nanowire device surface modification
● **TIMING 5–6 h**
34| Clean a sensor device chip using an oxygen plasma: 30 W and 50 sccm O_2 for 60 s. The plasma-cleaned chip should be used promptly.
▲ **CRITICAL STEP** It is important to obtain clean, oxidized nanowire device surfaces for effective chemical modification in later steps.

35| Prepare silane/ethanol solution (1% v/v 3-(trimethoxysilyl)propyl aldehyde in ethanol/H_2O (95%/5%)) and allow to stand for 20 min before filtering with a 0.2 μm cut-off syringe filter. Immerse the plasma-cleaned sensor chip in the silane/ethanol solution for 30 min (**Fig. 11**).

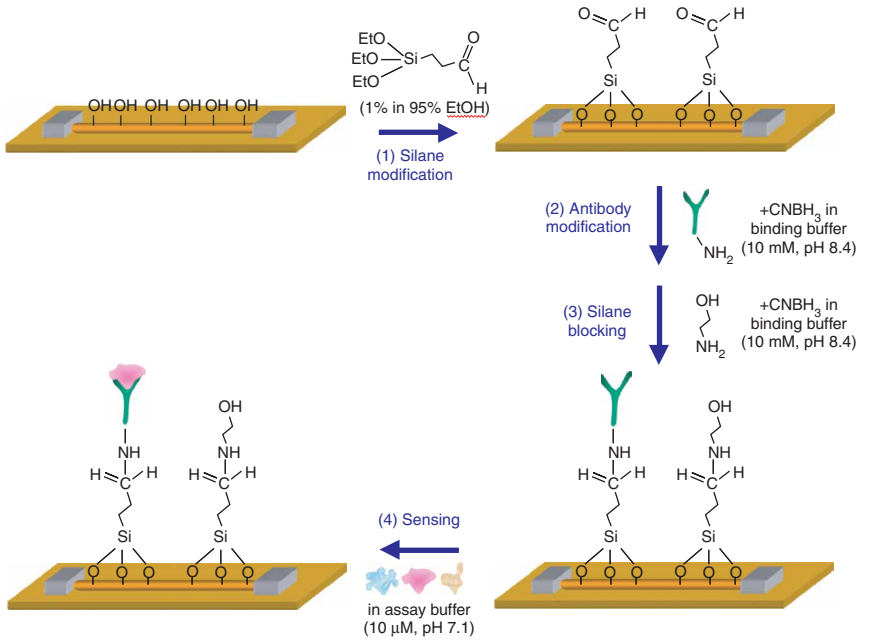

Figure 11 | Schematic of antibody modification, including: (1) aldehyde-silane modification; (2) antibody modification; (3) silane passivation by ethanolamine; and (4) sensing measurement.

36| Wash the sensor chip with ethanol flow for 50 s, dry in a stream of nitrogen gas and heat at 110 °C for 10 min. The silanized surfaces should be used as soon as possible after preparation, and kept under a dry nitrogen atmosphere until use if stored.

37| Mount the aldehyde-silane-modified SiNW sensor chip on the chip carrier using double-sided conductive carbon tape, and then use wire bonding to connect contact pads of good devices to the 24 output pads of the chip carrier (**Fig. 8b–d**).

38| Clamp a single channel microfluidic device on the chip carrier such that the channel overlaps the central region of the sensor chip, which contains the SiNW devices (**Fig. 8c,d**).

39| Draw a solution of monoclonal anti-PSA antibody receptor (10–100 μg ml^{-1} antibody in 10 mM phosphate buffer solution, pH 8.4, containing 4 mM sodium cyanoborohydride) into the PDMS channel and allow to react for 2–3 h at room temperature. (Note that anti-PSA is an example of modification for any antibody or protein receptor with an accessible lysine residue or other receptor with free amine group; see Experimental overview.)
? TROUBLESHOOTING

40| Wash the surface using a continuous flow of 10 mM phosphate buffer, pH 8.4, through the channel for 10 min.

41| Passivate unreacted aldehyde surface groups by drawing a solution of ethanolamine (100 mM ethanolamine in 10 mM phosphate buffer, pH 8.4) in the presence of 4 mM cyanoborohydride into the channel and allow to stand for 1-2 h (**Fig. 11**).
▲ **CRITICAL STEP** The coupling of ethanolamine prevents nonspecific adsorption of sample species on the nanowire surface during the course of sensing experiments; it is an essential step in the overall surface modification procedure.

42| Finally, wash the surface using a continuous flow of 10 mM phosphate buffer, pH 8.4, through the channel for 10 min. The sensor chip is now ready for detection experiments.

? TROUBLESHOOTING
For troubleshooting advice see **Table 1**.

© 2006 Nature Publishing Group http://www.nature.com/natureprotocols

TABLE 1 | Troubleshooting table.

Step	Problem	Solution
8	Nanowire growth is not uniform.	Non-uniform growth of nanowires over growth chips indicates that gold nanoparticles are not evenly dispersed. Test gold nanoparticle dispersion by SEM imaging, and correct by modifying plasma cleaning of growth-chip and/or poly-L-lysine adsorption. Non-uniform nanowire diameters indicate radial growth simultaneously with axial elongation. This condition must be corrected, because it will lead to non-uniform and irreproducible electronic properties. To correct, reduce growth temperature and/or total pressure until uniform diameters are observed.
9	Nanowire solutions contain substantial particles.	Do not sonicate for too long when preparing solution because the sonication process will fragment nanowires. Shorten sonication time if predominantly short (<10 μm) nanowires and/or particles are observed.
18	Nanowires are not evenly distributed on the sensor chip.	Use freshly prepared nanowire solution for deposition. Solutions ≤ 2 weeks old generally produce good results. Older solutions yield aggregates of nanowires on the sensor chip surface (**Fig. 5c,d**).
28	Sensor chips have poorly defined and/or broken metal lines, and a low yield of single nanowire devices.	Repeat and optimize photolithography exposure, developing and lift-off to achieve clean and unbroken metal lines. Use fresh nanowire solution and ensure that they are uniformly dispersed in appropriate region of device chip with correct density to achieve a high yield of single nanowire devices.
30	SiNW electrical measurements show low I_{ds} levels and/or non-linear I_{ds} increase with increasing V_{ds}.	Most common problems arise from poor electrical contacts. Repeat sensor chip fabrication paying careful attention to cleaning and etching immediately before Ni metal deposition. In addition, lift-off and subsequent annealing should be carried out promptly once the sensor chip is completed.
33	SiNW electrical data is unstable.	Unstable conductance (or I_{ds}) typically arises from inadequate passivation of the Ni-metal source and drain contacts with Si_3N_4, because Ni can undergo electrochemical corrosion in aqueous solution. To solve, repeat PE–CVD step in fabrication being sure to use the two-layer photoresist and stated parameters for the plasma deposition. If a different PE–CVD instrument is used, it may be necessary to optimize the deposition (varying power) until a conformal coating of the Ni metal is observed.
39	Antibody is not coupled in good yield to the SiNW surface.	Do not use antibody or protein solutions containing BSA as preservative since it will react with and block the nanowire surface. In addition, sodium azide, if present, must be removed before modification.

© 2006 Nature Publishing Group http://www.nature.com/natureprotocols

ANTICIPATED RESULTS

The sensor chips can be used for a variety of electrically based detection experiments as outlined in the INTRODUCTION. Three different examples of typical results obtained using different sensor chip configurations for the detection of prostate-specific antigen (PSA) using monoclonal anti-PSA antibody–modified SiNWs described above are shown in **Figure 12**. In these experiments, the conductance (G) of SiNW devices is continuously measured using lock-in detection (see Step 33 and **Fig. 8**), and the resulting signal is digitized and displayed or saved on a computer as different solutions are sequentially drawn into the microfluidic channel using the syringe pump. Up to 16 devices can be simultaneously digitized using the digital–analog converter specified in this protocol.

Concentration-dependent binding behavior can be readily assessed. PSA of varying concentration and buffer solutions are sequentially drawn through the microfluidic channel while monitoring the conductance of a SiNW device modified with anti-PSA. Conductance versus time data (**Fig. 12a**) show well-defined conductance increases and subsequent returns to baseline as the PSA and pure buffer solutions, respectively, are delivered through a microfluidic channel to the device. These data show that direct label-free detection of PSA is achieved with signal-to-noise >3 for concentrations down to 90 fg ml^{-1} or ~ 2.5 fM.

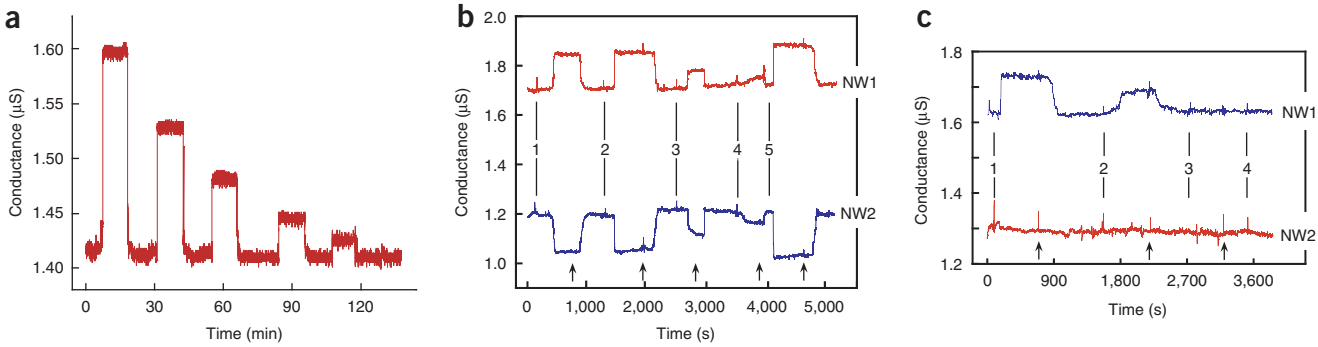

Figure 12 | Real-time nanowire sensing results. (**a**) Conductance versus time data recorded following alternate delivery of PSA and pure buffer solutions; the PSA concentrations were 5 ng ml^{-1}, 0.9 ng ml^{-1}, 9 pg ml^{-1}, 0.9 pg ml^{-1} and 90 fg ml^{-1}, respectively. The buffer solutions used in all measurements were 1 μM phosphate (potassium salt) containing 2 μM KCl, pH 7.4. (**b**) Complementary sensing of PSA using p-type (NW1) and n-type (NW2) nanowire devices. Vertical lines correspond to addition of PSA solutions of (1,2) 0.9 ng ml^{-1}, (3) 9 pg ml^{-1}, (4) 0.9 pg ml^{-1} and (5) 5 ng ml^{-1}. Arrows on the bottom represent the injections of sensing buffer solution. (**c**) Conductance versus time data recorded simultaneously from two p-type silicon nanowire devices in an array, where NW1 was functionalized with PSA Ab1, and NW2 was modified with ethanolamine. The vertical lines correspond to times when solutions of (1) 9 pg ml^{-1} PSA, (2) 1 pg ml^{-1} PSA, (3) 10 μg ml^{-1} BSA, (4) a mixture of 1 ng ml^{-1} PSA and 10 μg ml^{-1} PSA Ab1 were delivered to the microfluidic channel. Black arrows in **b** and **c** indicate switch of solution flow from protein to pure buffer solution.

In addition, two types of multiplexing experiments are shown to illustrate methods of guarding against false-positive binding events. First, a sensor chip containing both p-type and n-type SiNW devices was modified with anti-PSA. Simultaneous conductance versus time data recorded from p-type nanowire (NW1) and n-type nanowire (NW2) devices as PSA and buffer solutions are delivered through the microfluidic channel to the devices exhibit time correlated increases and decreases for the p-type and n-type devices, respectively, as shown in **Figure 12b**. The incorporation of p- and n-type nanowires in a single sensor chip enables electrical cross-talk and/or false positive signals to be discriminated by correlating the response versus time from the two distinct types of device elements.

A second example of multiplexing involves a sensor chip in which p-type SiNW devices are functionalized with anti-PSA (NW1) or ethanolamine (NW2). Simultaneous measurements of the conductance show that well-defined concentration-dependent conductance increases are only observed in NW1 upon delivery of PSA solutions through the microfluidic channel (9 and 1 pg ml^{-1}), and that delivery of BSA at 10 μg ml^{-1} showed no conductance change in either NW1 or NW2 (**Fig. 12c**). These multiplexing experiments demonstrate that the electronic signals measured using SiNW sensor chips can be readily attributed to selective protein binding; show that the surface passivation chemistry effectively prevents nonspecific protein binding; and also provide a robust means for discriminating against false-positive signals arising from either electronic noise or nonspecific binding.

© 2006 Nature Publishing Group http://www.nature.com/natureprotocols

COMPETING INTERESTS STATEMENT The authors declare that they have no competing financial interests.

Published online at http://www.natureprotocols.com
Rights and permissions information is available online at http://npg.nature.com/reprintsandpermissions

1. Morales, A.M. & Lieber, C.M. A laser ablation method for the synthesis of crystalline semiconductor nanowires. *Science* **279**, 208–211 (1998).
2. Lieber, C.M. Nanoscale science and technology: Building a big future from small things. *MRS Bull.*, **28**, 486–491 (2003).
3. Xiang, J. *et al.* Ge/Si nanowire heterostructures as high-performance field-effect transistors. *Nature* **441**, 489–493 (2006).
4. Cui, Y., Zhong, Z., Wang, D., Wang, W.U. & Lieber, C.M. High performance silicon nanowire field effect transistors. *Nano Lett.* **3**, 149–152 (2003).
5. Jin, S. *et al.* Scalable interconnection and integration of nanowire devices without registration. *Nano Lett.* **4**, 915–919 (2004).
6. Patolsky, F. & Lieber, C.M. Nanowire nanosensors. *Mater. Today* **8**, 20–28 (2005).
7. Cui, Y., Wei, Q., Park, H. & Lieber, C.M. Nanowire nanosensors for highly sensitive and selective detection of biological and chemical species. *Science* **293**, 1289–1292 (2001).
8. Sze, S.M. *Physics of Semiconductor Devices* Edn. 2 p. 481 (John Wiley & Sons, New York, 1981).
9. Domansky, K. & Janata, J. Present state of fabrication of chemically sensitive field-effect transistors. *Analyst* **118**, 335–340 (1993).
10. Janata, J. 20 Years of ion-selective field-effect transistors. *Analyst* **119**, 2275–2278 (1994).
11. Hahm, J. & Lieber, C.M. Direct ultrasensitive electrical detection of DNA and DNA sequence variations using nanowire nanosensors. *Nano Lett.* **4**, 51–54 (2004).
12. Wang, W.U., Chen, C., Lin, K.H., Fang, Y. & Lieber, C.M. Label-free detection of small-molecule-protein interactions by using nanowire nanosensors. *Proc. Natl. Acad. Sci. USA* **102**, 3208–3212 (2005).
13. Patolsky, F. *et al.* Electrical detection of single viruses. *Proc. Natl. Acad. Sci. USA* **101**, 14017–14022 (2004).
14. Zheng, G.F., Patolsky, F., Cui, Y., Wang, W.U. & Lieber, C.M. Multiplexed electrical detection of cancer markers with nanowire sensor arrays. *Nat. Biotechnol.* **23**, 1294–1301 (2005).
15. Hu, J.T., Odom, T.W. & Lieber, C.M. Chemistry and physics in one dimension: Synthesis and properties of nanowires and nanotubes. *Acc. Chem. Res.* **32**, 435–445 (1999).
16. Cui, Y., Lauhon, L.J., Gudiksen, M.S., Wang, J. & Lieber, C.M. Diameter-controlled synthesis of single-crystal silicon nanowires. *Appl. Phys. Lett.* **78**, 2214–2216 (2001).
17. Wu, Y. Controlled growth and structures of molecular-scale silicon nanowires. *Nano Lett.* **4**, 433–436 (2004).
18. Zheng, G.F., Lu, W., Jin, S. & Lieber, C.M. Synthesis and fabrication of high-performance n-type silicon nanowire transistors. *Adv. Mater.* **16**, 1890–1893 (2004).
19. Iler, R.K. *The Chemistry of Silica: Solubility, Polymerization, Colloid and Surface Properties and Biochemistry of Silica* (John Wiley & Sons, New York, 1979).

20. Ward, A.M., Catto, J.W.F. & Hamdy, F.C. Prostate specific antigen: biology, biochemistry and available commercial assays. *Ann. Clin. Biochem.* **38**, 633–651 (2001).
21. Mirkin, C.A. *et al.* A DNA-based method for rationally assembling nanoparticles into macroscopic materials. *Nature* **382**, 607–609 (1996).
22. Campagnolo, C. *et al.* Real-Time, label-free monitoring of tumor antigen and serum antibody interactions. *J. Biochem. Biophys. Methods* **61**, 283–298 (2004).
23. Wu, G.H. *et al.* Bioassay of prostate-specific antigen (PSA) using microcantilevers. *Nat. Biotechnol.* **19**, 856–860 (2001).
24. Chen, R.J. *et al.* Noncovalent functionalization of carbon nanotubes for highly specific electronic biosensors. *Proc. Natl. Acad. Sci. USA* **100**, 4984–4989 (2003).
25. Patolsky, F., Zheng, G.F. & Lieber, C.M. Nanowire sensors for medicine and the life sciences. *Nanomedicine* **1**, 51–65 (2006).
26. Patolsky, F., Zheng, G.F. & Lieber, C.M. Nanowire-based biosensors. *Anal. Chem.* **78**, 4261–4269 (2006).
27. Becker, J. Signal transduction inhibitors – a work in progress. *Nat. Biotechnol.* **22**, 15–18 (2004).
28. Patolsky, F. *et al.* Detection, stimulation and inhibition of neuronal signals with high-density nanowire transistor arrays. *Science* **313**, 1100–1104 (2006).
29. MacBeath, G. & Schreiber, S.L. Printing proteins as microarrays for high-throughput function determination. *Science* **289**, 1760–1763 (2000).
30. Whitesides, G.M., Ostuni, E., Takayama, S., Jiang, X. & Ingber, D.E. Soft lithography in biology and biochemistry. *Annu. Rev. Biomed. Eng.* **3**, 335 (2001).
31. Huang, Y., Duan, X.F., Wei, Q.Q. & Lieber, C.M. Directed assembly of one-dimensional nanostructures into functional networks. *Science* **291**, 630–633 (2001).
32. Whang, D., Jin, S. & Lieber, C.M. Large-scale hierarchical organization of nanowires for functional nanosystems. *Japan. J. Appl. Phys.* **43**, 4465–4470 (2004).
33. Wu, Y., Xiang, J., Yang, C., Lu, W. & Lieber, C.M. Single-crystal metallic nanowires and metal/semiconductor nanowire heterostructures. *Nature* **430**, 61–65 (2004).

© 2006 Nature Publishing Group http://www.nature.com/natureprotocols